Ultrathin, Hyperbranched Poly(acrylic acid) Membranes on Porous Alumina Supports

Milind Nagale, Bo Young Kim, and Merlin L. Bruening*

Contribution from the Department of Chemistry and Center for Fundamental Materials Research, Michigan State University, East Lansing, Michigan 48824

Received June 19, 2000

Abstract: The synthesis of high-flux composite membranes requires deposition of an ultrathin, discriminating layer on a highly permeable support. This paper describes the synthesis, derivatization, and characterization of hyperbranched poly(acrylic acid) (PAA) membranes on porous alumina supports. PAA films as thin as ∼40 nm effectively cover underlying pores without filling them, presumably because of their hyperbranched structure. Synthesis of these films begins by sputtering a thin gold layer on the alumina support and then grafting a layer of PAA to a self-assembled monolayer of mercaptoundecanoic acid on the gold. Graft-on-graft deposition of PAA yields the hyperbranched membrane. FESEM (field-emission scanning electron microscopy) and AFM (atomic force microscopy) images clearly show that hyperbranched PAA films can completely cover the substrate surface without filling underlying pores, thus creating an ultrathin membrane on a porous support. PAA membranes are especially attractive because derivatization permits control over transport properties. Gas transport studies indicate that three-layer PAA films do not show a high selectivity by themselves, but selectivity improves significantly after covalent derivatization of PAA with $H_2NCH_2(CF_2)_6CF_3$.

Introduction

Although membrane separations are attractive because of low energy costs and simple operation, low permeabilities and/or selectivities often limit membrane applications.[1−4] Successful commercial applications of membrane separations already include production of nitrogen from air and recovery of hydrogen from mixtures having other larger components such as nitrogen, methane, and carbon monoxide.[5] Improvements in throughput and selectivity, however, could greatly increase the impact of membrane separations.[6]

One major limitation of gas-separation membranes is that selective materials are generally not highly permeable.[7−9] This tradeoff between selectivity and permeability makes decreasing membrane thickness vital for increasing flux without sacrificing selectivity.[3,10,11] As shown in equation 1, gas flux through a membrane is inversely proportional to membrane thickness (l) and directly proportional to the pressure gradient across the membrane (Δp) and the permeability coefficient (P) for a specific gas.[12]

$$F = \frac{P\Delta p}{l} \tag{1}$$

The mechanical weakness of ultrathin films necessitates their deposition on highly permeable supports that provide strength. Unfortunately, synthesis of defect-free ultrathin (<50 nm) membrane "skins" is challenging.[3,11,13]

There are several approaches to preparing membranes with ultrathin skins. One strategy involves phase-inversion to prepare an asymmetric membrane from a single material. The first asymmetric gas-separation membrane was a Loeb-Sourirajan-type cellulose acetate (CA) membrane formed by drying CA membranes using quick-freezing and vacuum sublimation at −10 °C.[14] More recent efforts include synthesis of integrally skinned membranes using a dry/wet-phase inversion process.[13] Asymmetric carbon molecular sieve membranes can even be prepared by formation of a capillary type polyamic acid membrane followed by imidization and pyrolysis to form a dense selective layer supported by a porous layer.[15]

Composite membranes provide a versatile alternative to asymmetric skinned systems. In this case a polymer skin is deposited on a separate, highly permeable support. Composite membranes have the advantage that only a small amount of a possibly expensive skin material needs to be used. Strategies for forming the skins of these membranes include casting,[16,17] in situ casting,[18] in situ condensation of polymers and/or

* To whom correspondence should be addressed. Phone: (517) 355-9715, ext. 237. Fax: (517) 353-1793. E-mail: bruening@cem.msu.edu.

(1) Abelson, P. H. *Science* **1989**, *244*, 1421.
(2) Henis, J. M. S.; Tripodi, M. K. *Science* **1983**, *220*, 11−17.
(3) Haggin, J. *Chem. Eng. News* **1990**, *68*, 22−26.
(4) Spillman, R. W. *Chem. Eng. Prog.* **1989**, *85*, 41−62.
(5) Freeman, B. D.; Pinnau, I. In *Polymer Membranes for Gas and Vapor Separation*; Freeman, B. D., Pinnau, I., Eds.; ACS Symposium Series 733; American Chemical Society: Washington, DC, 1999; pp 1−27.
(6) Maier, G. *Angew. Chem., Int. Ed. Engl.* **1998**, *37*, 2960−2974.
(7) Freeman, B. D. *Macromolecules* **1999**, *32*, 375−380.
(8) Robeson, L. M. *J. Membr. Sci.* **1991**, *62*, 165−185.
(9) Robeson, L. M.; Burgoyne, W. F.; Langsam, M.; Savoca, A. C.; Tien, C. F. *Polymer* **1994**, *35*, 4970−4978.
(10) Rezac, M. E.; Koros, W. J. *J. Appl. Polym. Sci.* **1992**, *46*, 1927−1938.
(11) Liu, C.; Martin, C. R. *Nature* **1991**, *352*, 50−52.
(12) Prasad, R.; Shaner, R. L.; Doshi, K. J. In *Polymeric Gas Separation Membranes*; Paul, D. R., Yampol'skii, Y. P., Eds.; CRC Press: Boca Raton, 1994; pp 513−614.
(13) Pinnau, I.; Koros, W. J. *Ind. Eng. Chem. Res.* **1991**, *30*, 1837−1840.
(14) Gantzel, P. K.; Merten, U. *I&EC Proc. Des. Dev.* **1970**, *9*, 331.
(15) Suda, H.; Haraya, K. In *Membrane Formation and Modification*; Pinnau, I., Freeman, B. D., Eds.; ACS Symposium Series 744; American Chemical Society: Washington, DC, 2000; pp 295−313.
(16) Francis, P. *Fabrication and Evaluation of New Ultrathin Reverse Osmosis Membranes*; NTIS Report, Pb-177083, Springfield, VA, 1966.
(17) Le Roux, J. D.; Paul, D. R. *J. Membr. Sci.* **1992**, *74*, 233−252.

10.1021/ja002203t CCC: $19.00
Published on Web 11/08/2000

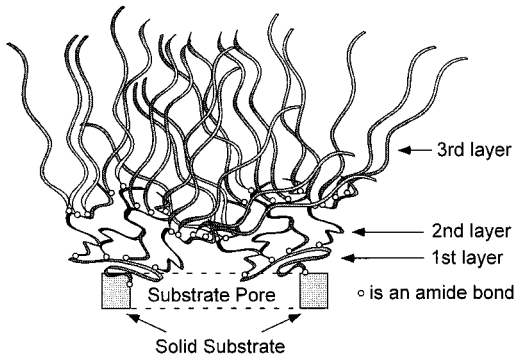

Figure 1. Idealized cartoon of a hyperbranched PAA film grafted onto a porous alumina substrate. Substrate thickness is not drawn to scale.

monomers at the porous support,[19] and plasma polymerization.[20] In all of these methods, synthesis of defect-free skins with thicknesses <50 nm is difficult.

A few recent reports demonstrate that composite membranes with ultrathin skins are capable of selective separations. With the thinnest synthetic gas-separation membranes to date, Regen and co-workers showed that Langmuir−Blodgett films as thin as a single monolayer can serve as selective membranes when deposited on a continuous, glassy, polymer support.[21−23] Liu and Martin reported fabrication of ultrathin, conducting, polymer membranes (∼50 nm thick) with an O_2/N_2 selectivity of 8.[11] In this case interfacial photopolymerization at the alumina surface resulted in an ultrathin conducting polymer membrane. Similar selectivities can be achieved by electrochemical synthesis of ultrathin films on porous alumina membranes.[24] Thin film composite membranes can also be formed on hollow fibers. Paul et al. formed multilayered, composite, hollow-fiber membranes by dip-coating hollow-fiber polysulfone supports with a selective poly(4-vinylpyridine) layer (50−150 nm thick) and sealing them with a silicone rubber layer. This system has a selectivity of 7 for O_2/N_2.[25]

We report fabrication of surface-grafted, hyperbranched, poly(acrylic acid) (PAA) membranes. These films are unique in that their highly branched structure allows them to cover underlying pores without filling them, as shown schematically in Figure 1.[26] Additionally, in situ derivatization of these materials allows synthesis of a variety of membranes without the need to prepare new polymers. The synthesis of PAA membranes (Figure 2) involves first forming a self-assembled monolayer of a carboxylic acid-terminated thiol on a gold-coated porous substrate followed by the conversion of carboxylates to mixed anhydrides. These mixed anhydrides are then used as attachment points for the grafting of amine-terminated poly(*tert*-butyl acrylate) (PTBA) onto the surface. The hydrolysis of *tert*-butyl groups to carboxylic acid groups forms a PAA layer, and the whole process is then repeated to graft additional layers to the immobilized PAA. The layer-by-layer synthesis of hyperbranched PAA affords control over film thickness, while derivatization of the films provides a way to chemically control transport properties.[26] Derivatization occurs through amidation or esterification of the −COOH groups of PAA with functional amines or alcohols, and prior studies show that PAA films can be modified to give fluorescent, hydrophobic, ion-binding, biocompatible, and electroactive films.[27] Thus, derivatizaton can provide a wide variety of hyperbranched membranes for investigating relationships between transport and membrane chemistry. This paper focuses on derivatization of hyperbranched PAA by $H_2NCH_2(CF_2)_6CF_3$ because this procedure produces selective gas-separation membranes. The occurrence of gas selectivity shows that these ultrathin membranes are free of defects.

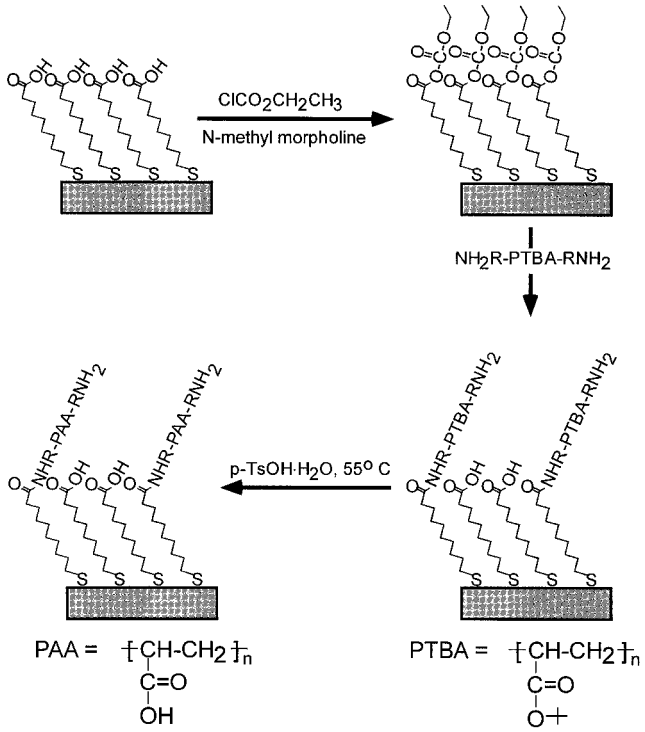

Figure 2. Schematic diagram of the synthesis of 1 layer of PAA on a surface. Additional layers were prepared by grafting onto previously deposited PAA.

Experimental Section

Materials. Porous alumina (0.02 and 0.2 μm pore diameter Anopore filters) substrates were purchased from Thomas Scientific. Ethyl chloroformate (97%), *N*-methyl morpholine (99%), *p*-toluenesulfonic acid monohydrate (98%), 4,4′-azobis(4-cyanovaleric acid) (75%+), 1,4-dioxane (99%), and *tert*-butyl acrylate (98%) were purchased from Aldrich. $H_2NCH_2(CF_2)_6CF_3$ (97%) was purchased from Lancaster. Acetonitrile (Spectrum, 99.5%), and ethanol (Pharmco, 100%) were used as received. DMF (Aldrich, 99.9%) was dried with molecular sieves for 24 h before use, and deionized water (18.2 MΩ·cm) was obtained using a Milli-Q system. Mercaptoundecanoic acid (MUA) was initially synthesized using a modified literature procedure,[28] but most of the MUA used in this research was purchased from Aldrich. α,ω-Diamino-terminated poly(*tert*-butyl acrylate) ($H_2NR-PTBA-RNH_2$), R = $(CH_2)_2NHCO(CH_2)_2C(CN)(CH_3)$, was prepared according to a

(18) Kesting, R. *Synthetic Polymeric Membranes: A Structural Perspective*; John Wiley & Sons: New York, 1985; pp 224−236.
(19) Cadotte, J. In *Materials Science of Synthetic Membranes*; Lloyd, D. R., Ed.; ACS Symposium Series 269; American Chemical Society: Washington, DC, 1985; pp 273−294.
(20) Kesting, R. E.; Fritzsche, A. K. *Polymeric Gas Separation Membranes*; John Wiley & Sons: New York, 1993; pp 284−318.
(21) Conner, M. D.; Janout, V.; Kudelka, I.; Dedek, P.; Zhu, J.; Regen, S. L. *Langmuir* **1993**, *9*, 2389−2397.
(22) Hendel, R. A.; Nomura, E.; Janout, V.; Regen, S. L. *J. Am. Chem. Soc.* **1997**, *119*, 6909−6918.
(23) Zhang, L.-H.; Hendel, R. A.; Cozzi, P. G.; Regen, S. L. *J. Am. Chem. Soc.* **1999**, *121*, 1621−1622.
(24) Liu, C.; Chen, W. J.; Martin, C. R. *J. Membr. Sci.* **1992**, *65*, 113−128.
(25) Shieh, J. J.; Chung, T. S.; Paul, D. R. *Chem. Eng. Sci.* **1999**, *54*, 675−684.
(26) Zhou, Y.; Bruening, M. L.; Bergbreiter, D. E.; Crooks, R. M.; Wells, M. *J. Am. Chem. Soc.* **1996**, *118*, 3773−3774.
(27) Bruening, M. L.; Zhou, Y.; Aguilar, G.; Agee, R.; Bergbreiter, D. E.; Crooks, R. M. *Langmuir* **1997**, *13*, 770−778.
(28) Odukale, A. A. M.S. Thesis, Michigan State University, 1999.

literature procedure.[26,27] He (99.995%), N_2 (99.99%), O_2 (99.99%), CO_2 (99.8%), CH_4 (99.3%), and SF_6 (99.99%) were purchased from AGA.

Synthesis of PAA Films. Alumina substrates were cleaned for 10 min in a UV/ozone cleaner (Boekel Industries, model 135500) after a 10 min immersion in boiling methanol. Subsequently, gold (63 or 5 nm) was sputtered (Ted Pella, Pelco SC-7) onto the substrates. Sputtering was performed using a current of 20 mA and a pressure of ~0.08 mbar (Ar plasma) at a rate of 1 Å/s. Gold-coated porous alumina substrates were cleaned in the UV/ozone cleaner for 12 min before beginning monolayer deposition.

To synthesize PAA films, we grafted $H_2NR-PTBA-RNH_2$ via amide formation onto a mercaptoundecanoic acid (MUA) monolayer attached to gold-coated porous alumina. Hydrolysis of *tert*-butyl ester groups with *p*-toluenesulfonic acid results in a grafted PAA film. Repeating these steps using additional grafting at multiple sites on each prior graft produces layered, hyperbranched polymer membranes. This procedure was described previously.[26]

Derivatization of 3-Layer PAA Films. After synthesis of three-layer PAA membranes and measurement of their gas permeability, these films were derivatized with $H_2NCH_2(CF_2)_6CF_3$. To derivatize PAA membranes, the film was first activated using ethyl chloroformate in the presence of *N*-methylmorpholine to form mixed anhydrides. The film was rinsed using ethyl acetate, dried using N_2, soaked in a solution of 0.1 M $H_2NCH_2(CF_2)_6CF_3$ in DMF for 1 h, rinsed using ethanol, and dried using nitrogen.[29]

Fourier Transform Infrared Spectroscopy. External reflection FTIR spectra of PAA films on substrates coated with 63 nm of gold were acquired using a Nicolet FTIR spectrometer (MAGNA 560) equipped with a MCT detector and a PIKE grazing angle accessory (incident angle of 80°, 256 scans at 4 cm^{-1} resolution). Transmission FTIR spectroscopy (Mattson Instruments, Infinity Gold) was employed to monitor the growth of hyperbranched PAA on alumina supports coated with only 5 nm of gold because these substrates are not sufficiently reflective for external reflection FTIR.

Field-Emission Scanning Electron Microscopy (FESEM). Electron microscope images of membranes were obtained using a Hitachi S-4700II field-emission scanning electron microscope. To prepare membrane cross-sections for imaging, samples were cleaved using tweezers, sputter-coated with 5 nm of gold, rinsed using methanol, and dried using nitrogen unless otherwise noted. In the cleaving process, a membrane was held by one pair of tweezers and bent with another pair to break the alumina support. The polymer support ring around the edge of the alumina was then cut away using a pair of scissors. During imaging, a low accelerating voltage (4 kV; beam current, 10 μA) was used to minimize the effects of sample charging and to provide better surface details.[30,31]

Atomic Force Microscopy (AFM). AFM images were obtained with a Nanoscope IIIa (Digital Instruments) using the tapping mode (scan rate = 1 Hz). A cantilever having a nominal spring constant of 20−100 N/m was used along with etched silicon tips. The tips have a nominal radius of curvature of 20−60 nm. Membranes could be directly imaged by AFM without any special preparation.

Gas-Transport Measurements. Gas-transport measurements were performed using a permeation cell (MKS Instruments, cell 02910-40) equipped with a pressure relief valve. Permeate flux was measured as a function of inlet pressure (10−40 psig) using a digital soap bubble flowmeter (Fisher Scientific, model 420). The area of the membrane exposed to the gas stream was 2.8 cm^2. The permeabilities of He, N_2, O_2, CO_2, CH_4, and SF_6 were determined for each sample. Three different membranes of each type were tested with at least three steady-state measurements of flux for each gas at a given pressure. The order in which the permeability of the various gases was determined was deliberately varied, and each sample was tested at least twice for the entire set of gases to check the stability of the membrane. The cell was purged several times using the gas of interest at a pressure of 50 psig using the pressure relief valve before performing any measurements with a particular gas. All measurements were obtained after the flux reached a steady-state value to ensure complete purging of the cell. After permeability measurements of membranes coated with PAA layers, the samples were removed, analyzed by transmission FTIR, and fluorinated as described in the synthesis section. The permeability of the fluorinated PAA layers was then measured.

Results and Discussion

Spectroscopic Characterization of PAA Membranes. Hyperbranched PAA films having up to six layers were synthesized on gold-coated porous alumina as shown in Figure 2, and the synthetic procedure was monitored by FTIR spectroscopy. In agreement with previous syntheses of hyperbranched PAA on gold-coated silicon wafers,[26] external-reflection FTIR spectra confirmed the steps of the synthetic process, including formation of a mixed anhydride, attachment of $H_2NR-PTBA-RNH_2$ to the surface, and hydrolysis of *tert*-butyl ester groups. External-reflection FTIR spectra of one to six layers of PAA grafted onto gold-coated (63 nm) porous alumina indicate that the absorbance due to the C=O band of PAA increases nonlinearly as a function of the number of layers, which suggests hyperbranched growth of these films (see Figure 1 of the Supporting Information for actual spectra.) We estimated the thickness of the PAA films on porous alumina by comparing their IR absorbances with absorbances due to films of known ellipsometric thickness on gold wafers. Using this method, the estimated thickness of a six-layer PAA film on porous alumina is about 940 Å.[32] This compares reasonably well with FESEM images, which show six-layer PAA films to be about 850 Å thick. Because alumina substrates are highly porous, direct ellipsometric measurements are not possible on these membranes.

We utilized transmission FTIR spectroscopy in an effort to investigate the synthesis of PAA films on porous alumina coated with 5 nm of gold because these surfaces are not sufficiently reflective for external-reflection FTIR spectroscopy. Large carbonyl absorbances in the transmission FTIR spectra of PAA-coated supports (absorbance of ~1.0 at 1712 cm^{-1} for six-layer films) suggest that considerable PAA is adsorbed inside the alumina pores. We confirmed this by control experiments where PAA films were grown with and without MUA monolayers on gold-coated (5 nm) alumina membranes. Absorbance values are comparable for the two cases, which indicates that growth inside the pores is the primary reason for the large IR absorbances.

It is not surprising that some PAA would be present in substrate pores because a minimal amount of adsorption will be amplified by hyperbranched growth. During the deposition of PTBA, some physisorption likely occurs. After hydrolysis, interaction of the $-COO^-$ groups of PAA with alumina may result in even stronger physisorption. The high internal surface area of the alumina supports leads to large carbonyl absorbances even when only a small fraction of the pores is filled with PAA. Comparison of IR absorbances of PAA films grown on alumina supports to absorbances of known amounts of PAA physisorbed on alumina supports indicates that there is 1.1 ± 0.4 mg of PAA distributed through alumina supports after the synthesis of a six-layer PAA film. The number of ~0.2 μm-diameter pores in the bulk of porous alumina is $2 \times 10^9/cm^2$ (determined from SEM images), giving a total internal surface area of 1800 cm^2

(29) Zhou, Y.; Bruening, M. L.; Liu, Y.; Crooks, R. M.; Bergbreiter, D. E. *Langmuir* **1996**, *12*, 5519−5521.

(30) Kim, K. J.; Dickson, M. R.; Chen, V.; Fane, A. G. *Micron Microsc. Acta* **1992**, *23*, 259−271.

(31) Coates, V. J. *Proc. 40th Ann. Electron Microsc. Soc. Am.* **1982**, 752−753.

(32) A hyperbranched PAA film (deposited on a gold wafer) with an ellipsometric thickness of 970 Å had a carbonyl absorbance of 0.113. Using this data point and the fact that the absorbance due to a six-layer PAA membrane on gold-coated alumina was 0.109, we estimated that the membrane thickness was 940 Å. Ellipsometric measurements on gold wafers were performed using a Woollam M-44 rotating analyzer ellipsometer. Substrate parameters (*n* and *k*) were determined prior to film deposition.

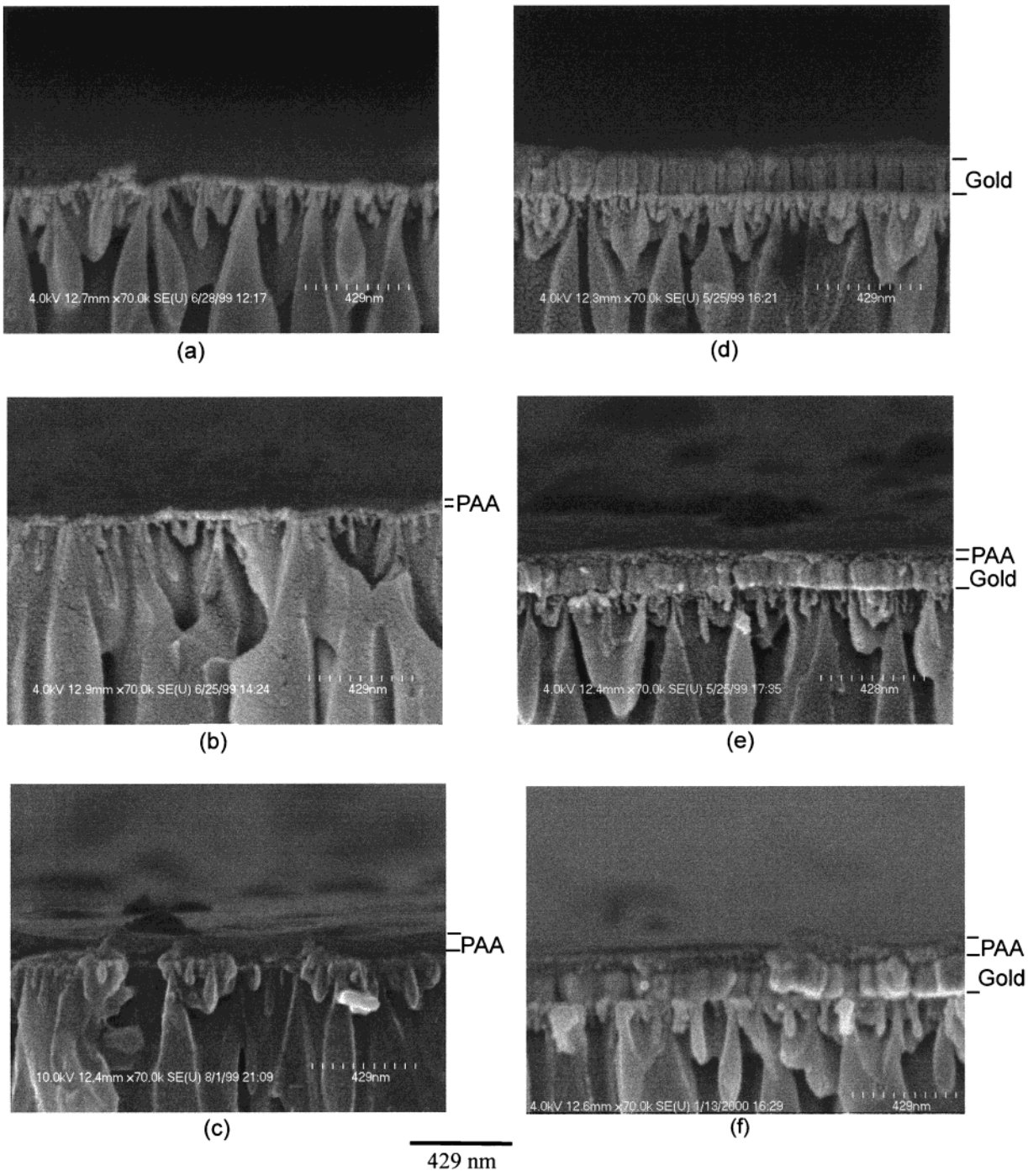

Figure 3. Field-emission scanning electron micrographs (cross-section) of porous alumina (0.02-μm pore diameter) before (a, d) and after deposition of four-layer (b, e) and six-layer (c, f) PAA films. In images a−c, 5 nm of gold was deposited before PAA growth, while in figures d−f, 63 nm of gold was deposited. After cleaving the membranes, samples were sputter-coated with 5 nm of gold for imaging.

for these 50 μm-thick membranes. If we assume that the PAA is distributed evenly across the internal surface area, there would be a 6 ± 2 nm-thick film along the pore walls. This would reduce the inside diameter of pores by <10%. For 3-layer PAA films, the pore diameter would hardly be affected. FESEM images and gas-permeability studies (vide infra) clearly show that PAA is not filling a substantial fraction of membrane pores.

Transmission FTIR spectroscopy confirms modification of three-layer PAA films with $H_2NCH_2(CF_2)_6CF_3$. After derivatization, the acid carbonyl peak (1712 cm^{-1}) diminishes and amide I (1669 cm^{-1}) and amide II (1537 cm^{-1}) bands appear. Additionally, a CF_X stretching peak appears at 1254 cm^{-1}. Other CF_X stretches cannot be observed because of the large absorbance of alumina below 1210 cm^{-1}. (See Figure 2 of the Supporting Information for actual spectra.) Although these spectra represent material both within the alumina and on its surface, similar chemistry should occur in both places.

Field-Emission Scanning Electron Microscopy (FESEM). Cross-sectional FESEM images of alumina supports before and after PAA growth indicate that PAA films cover substrate pores without filling them. Figure 3 shows FESEM images of porous alumina before and after coating with four- and six-layer PAA films. In the case of six-layer deposition, the PAA is easily observed, and yet, pores are unclogged. Because of their small thickness, four-layer PAA films are not easy to see. The large increase in film thickness on going from four to six layers

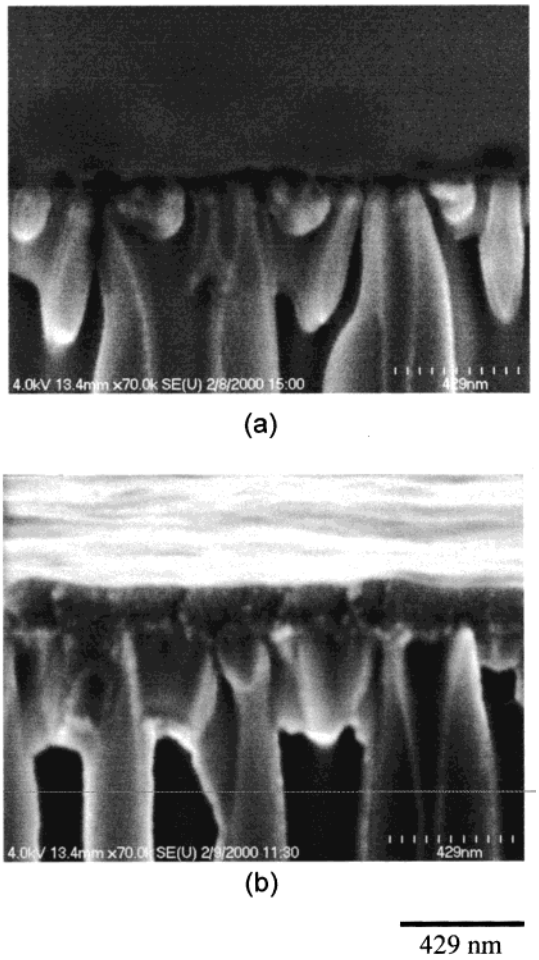

Figure 4. Field-emission scanning electron micrographs (cross-section) of porous alumina (0.2-μm pore diameter) before (a) and after (b) deposition of six PAA layers. Five nm of gold was deposited before PAA growth, and after cleaving, samples were sputter-coated with 5 nm of gold for imaging.

confirms the nonlinear PAA growth shown by FTIR. Prior to film synthesis, we sputter-coated the alumina with either 5 nm (a−c) or 63 nm (d−f) of gold. As seen by comparing images with no PAA films (a, d), the 63-nm gold layer is clearly distinguishable from the membrane and has a porous structure that does not form an impermeable barrier.

All of the images in Figure 3 were taken on substrates that have a nominal 0.02-μm pore diameter. These substrates have a very thin cake layer on their surface with 0.02 μm-diameter pores, while the bulk of the membrane has 0.2 μm-diameter pores. This substrate geometry makes it easier to cover pores without filling them. However, images of substrates with 0.2 μm-diameter pores (no cake layer) show that PAA films cover even these large pores (Figure 4). A PAA film is clearly visible after deposition of 6 layers on alumina coated with 5 nm of gold. Despite the larger pores, deposition is restricted primarily to the substrate surface.

In an effort to ensure that gold coating after cleavage does not affect the electron micrographs, we also imaged a sample covered with four layers of PAA (0.02-μm-diameter pores coated with 63 nm gold) without coating with gold after cleavage. (The actual image is given in Figure 3 of the Supporting Information.) The image shows the presence of PAA and confirms that the film is, in fact, PAA and not an artifact of sample preparation. FESEM images (cross-sections) of other types of control samples on which we attempted to graft six-layer PAA and fluorinated six-layer PAA films on gold-coated (5-nm) alumina without depositing a MUA monolayer do not show a significant film on the alumina surface. This is consistent with gas permeability data that show minimal inhibition of flux by membranes prepared without first depositing a layer of MUA.

Atomic Force Microscopy (AFM). AFM images show that six-layer PAA films completely cover the porous alumina surface. Figure 5 contains images of gold-coated porous alumina substrates before and after grafting four and six layers of hyperbranched PAA to the surface. With the addition of successive PAA layers, surface features of the porous alumina become less distinct as the film covers the substrate. Prior to PAA coating, images (a, d) show the pointed surface features of gold-coated alumina substrates. These images are similar to naked porous alumina. Interestingly, the sputtered gold appears to follow the pattern of the underlying substrate even when 63 nm of gold is deposited. This explains why the cross-sectional FESEM images show that thick gold coatings are porous. The pores in the alumina substrates most likely reside between the peaks on the surface. This topology allows hyperbranched PAA to effectively cover pores because the polymer can grow above the pore from all sides.

As the images show, covering the underlying alumina with PAA films greatly reduces surface roughness. To quantify changes in roughness, we used the instrument software to calculate average surface roughness values. Average roughness, R_a, is defined by equation 2

$$R_a = \frac{1}{N}\sum_{j=1}^{N} |Z_j| \qquad (2)$$

where Z_j is the deviation between the average surface height and the height at any point, and N is the number of points within the measured area. The surface of the alumina coated with 5 nm of gold has an average roughness of 40 ± 10 nm, while the surface of the alumina coated with 63 nm of gold has an average roughness of 19 ± 2 nm. In contrast, six-layer PAA surfaces on 5-nm gold-coated supports have average roughnesses of 7 ± 1 nm, and similar films on substrates coated with 63 nm of gold have average surface roughnesses of 6 ± 2 nm. These measurements show that six-layer PAA films form a smooth surface that covers underlying sharp features.

Figure 6 shows AFM images of PAA films that were prepared on gold-coated substrates with 0.2-μm-diameter surface pores. Pores in the substrate before coating with PAA (a, c) are an order of magnitude larger than those in Figure 5, as would be expected. After deposition of PAA, surface roughness decreased from 20 ± 2 nm to 9 ± 2 nm on the substrate coated with 5 nm of gold and from 18 ± 0.4 nm to 8 ± 1 nm on the surface coated with 63 nm of gold. The figure clearly shows that six layers of PAA completely cover underlying pores.

Defects in Gold Coatings. Selective transport requires defect-free films because flux through open channels will negate the selectivity of the membrane.[20] Unfortunately, during initial permeation studies we noticed that the 63-nm-thick gold coatings had small but visible holes. Careful inspection under a microscope revealed that there were at least 20 small (1−100 μm) holes in the gold layer on a substrate with an area of 3 cm^2. We inspected substrates under a microscope immediately after metal deposition, and most of the substrates had holes in the gold layer. Rinsing these samples with methanol and drying them with nitrogen produced additional holes. Optical microscope images often show that the small piece of gold removed from the surface by rinsing sits next to the newly formed hole.

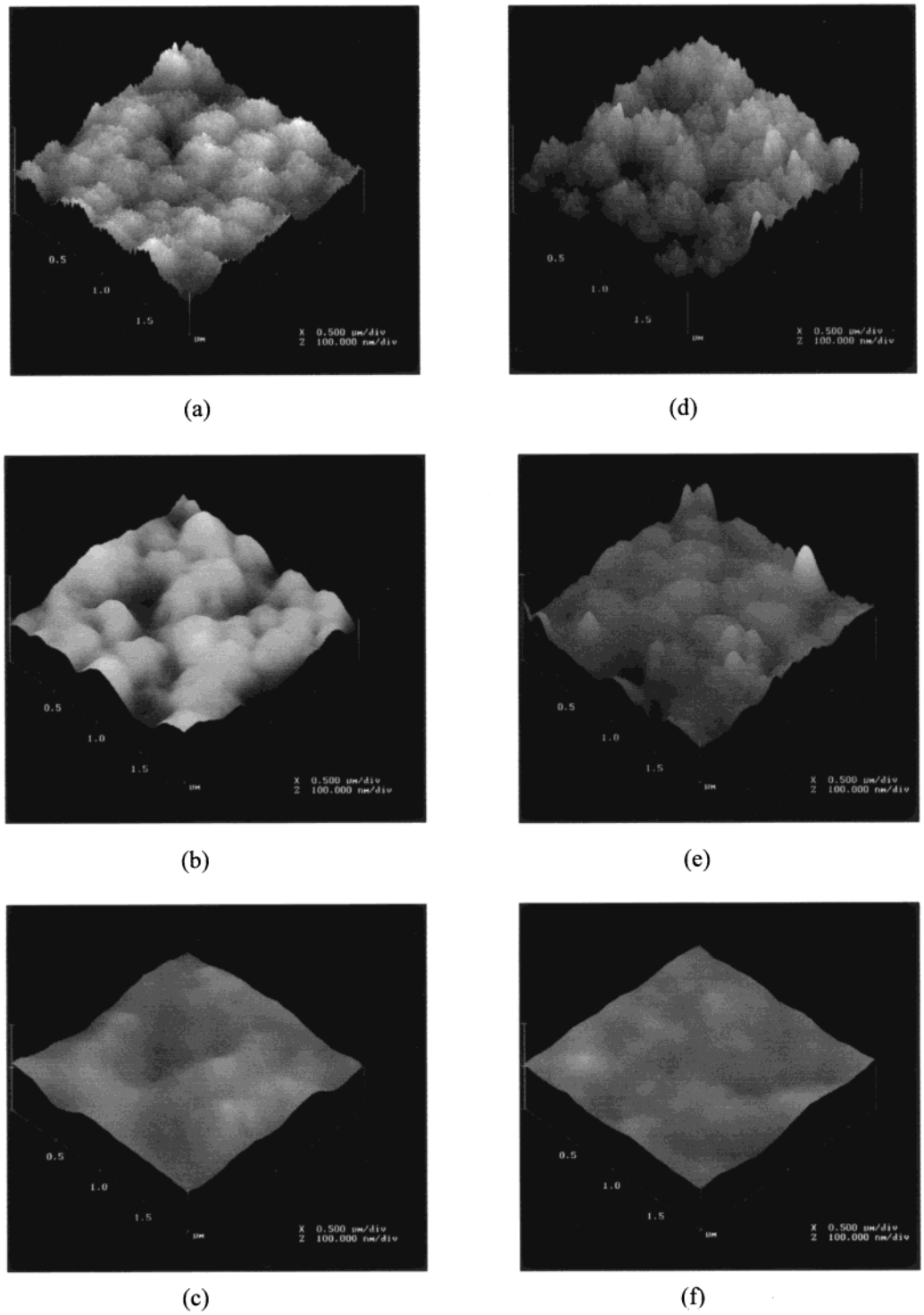

Figure 5. Tapping mode atomic force micrographs of gold-coated porous alumina substrates before (a, d) and after grafting of four-layer (b, e), and six-layer (c, f) PAA films. The gold coating on 0.02-μm pore diameter Anopore membranes was 5 nm thick in images a−c and 63 nm thick in images d−f.

Our attempts to improve adhesion of gold by cleaning with hot solvents, dilute ammonium hydroxide, UV/ozone, or Ar plasma did not provide a defect-free metal layer. The use of an adhesion layer (Cr or Ti) to prevent peeling was also unsuccessful. The only method that appeared to give a defect-free gold coating was deposition of a much thinner layer of gold (5 nm). We note, however, that it is more difficult to see defects in these thin gold coatings. Selectivities observed in gas-transport measurements (described below) give corroborating evidence that the 5-nm gold coating was free of defects.

Gas-Transport Measurements. In the solution-diffusion model of flux through a membrane, the permeability coefficient of a given analyte is related to its solubility and diffusion coefficient in the membrane material, as shown in equation 3,[5] where P is the permeability coefficient,

$$P = S \times D \tag{3}$$

S is the apparent solubility constant for the given gas−membrane pair, and D is the apparent diffusion coefficient. Selectivity is

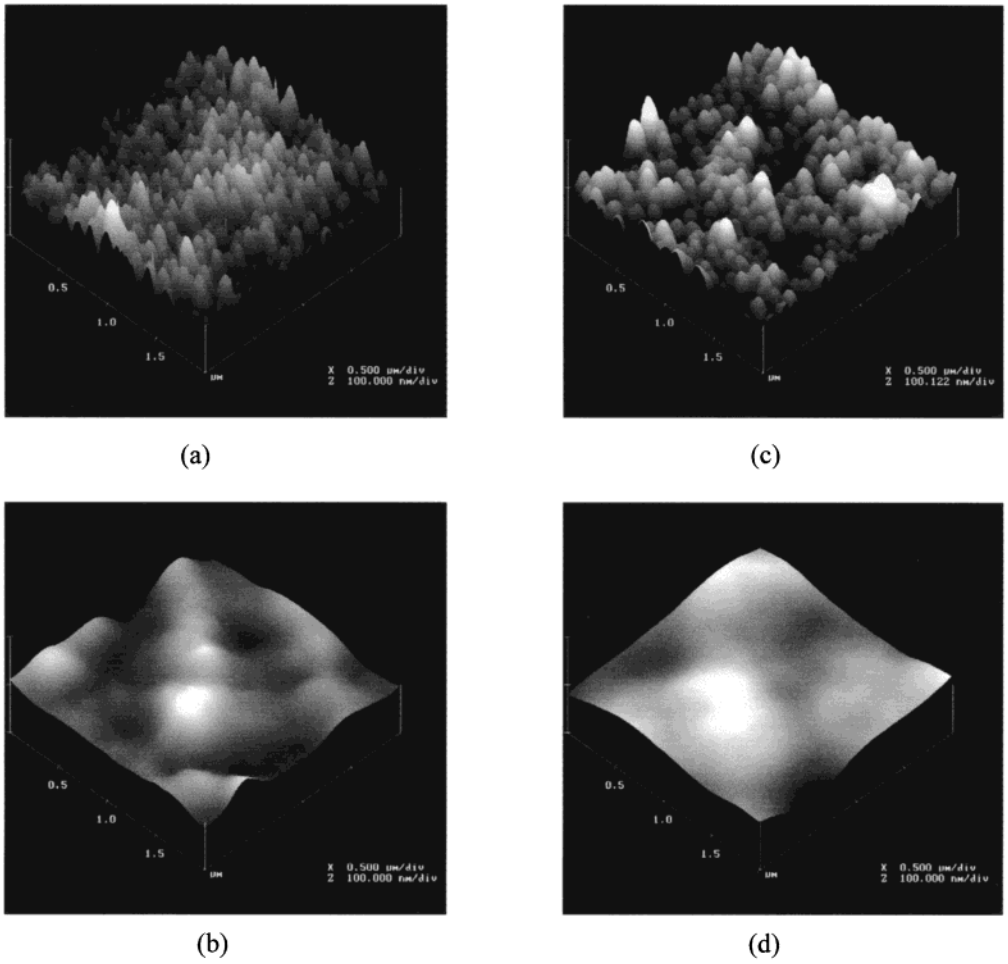

Figure 6. Tapping mode atomic force micrographs of gold-coated porous alumina substrates before (a,c) and after (b,d) the grafting of six layers of hyperbranched PAA. The gold coating on 0.2-μm pore diameter Anopore membranes was 5 nm thick in images a and b and 63 nm thick in images c and d.

defined as the ratio of the permeability coefficients of two different gases. Thus, selectivities between gases can result from differences in either solubility or diffusivity.

Using the 5-nm gold-coated substrate, we began investigating the gas permeability of three-layer hyperbranched PAA films. Figure 7 shows how gas flow through a three-layer PAA film varies according to inlet pressure for various gases. Total flux through these PAA membranes depends primarily on the molar mass of the gases; thus, He has the highest flux and SF_6 the lowest. The selectivity ratios are not very high and fall around or below calculated Knudsen diffusion values. Knudsen diffusion of gases results from diffusion through pores with radii that are much smaller than the mean free path of the gases, and flux is inversely proportional to the square root of molar mass.[20] These results suggest that three-layer PAA films are rather porous. We note, however, that the permeability of these membranes is orders of magnitude lower than the permeability of gold-coated porous alumina.

When PAA films were modified by fluorination with $H_2NCH_2(CF_2)_6CF_3$, selectivities improved significantly, and the relative fluxes did not depend solely on molar mass (Figure 8). The enhancement in selectivity occured because the permeability of some gases (He, O_2, and CO_2) increased upon fluorination, while other gases were relatively unaffected by derivatization. The selectivity ratios for several of the gas pairs are 3−4 times higher than those obtained with PAA films. Table 1 shows selectivity ratios for three-layer PAA and three-layer fluorinated PAA membranes, along with calculated values for Knudsen

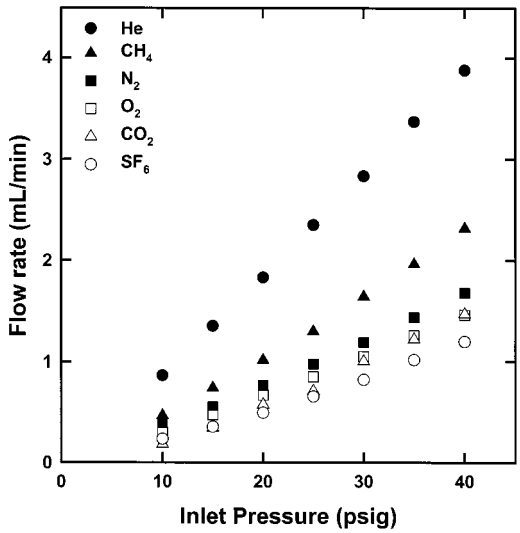

Figure 7. Flow rates of several gases through a three-layer PAA film on gold-coated (5 nm) porous alumina (0.02-μm pore diameter) as a function of inlet pressure. The membrane area was 2.8 cm^2. Permeability values with standard deviations are listed in the text.

diffusion-based selectivities. The increase in selectivity upon fluorination is not simply due to the filling of defects in the PAA films. If that were the case, flux would decrease for all gases and increases in flux for some of the gases upon fluorination certainly would not occur. Also, the addition of

Table 1. Ratios of the Flux of Different Gases through Three-Layer PAA Films and Fluorinated Three-Layer PAA Films[a]

	He	CH_4	N_2	O_2	CO_2	SF_6
He		1.3 (2.0) [6.7]	1.9 (2.6) [6.3]	2.0 (2.8) [2.8]	2.0 (3.3) [0.81]	2.4 (6.1) [24.4]
CH_4	1.3 (2.0) [6.7]		1.4 (1.3) [0.94]	1.5 (1.4) [0.42]	1.5 (1.7) [0.12]	1.8 (3.0) [3.6]
N_2	1.9 (2.6) [6.3]	1.4 (1.3) [0.94]		1.1 (1.1) [0.45]	1.1 (1.3) [0.13]	1.3 (2.3) [3.9]
O_2	2.0 (2.8) [2.8]	1.5 (1.4) [0.42]	1.1 (1.1) [0.45]		1.0 (1.2) [0.29]	1.2 (2.1) [8.6]
CO_2	2.0 (3.3) [0.81]	1.5 (1.7) [0.12]	1.1 (1.3) [0.13]	1.0 (1.2) [0.29]		1.2 (1.8) [30.0]
SF_6	2.4 (6.1) [24.4]	1.8 (3.0) [3.6]	1.3 (2.3) [3.9]	1.2 (2.1) [8.6]	1.2 (1.8) [30.0]	

[a]Values for fluorinated films are in brackets. The ratios for Knudsen-diffusion selectivity are given in parentheses. All values represent the flux of the lighter gas divided by the flux of the heavier gas.

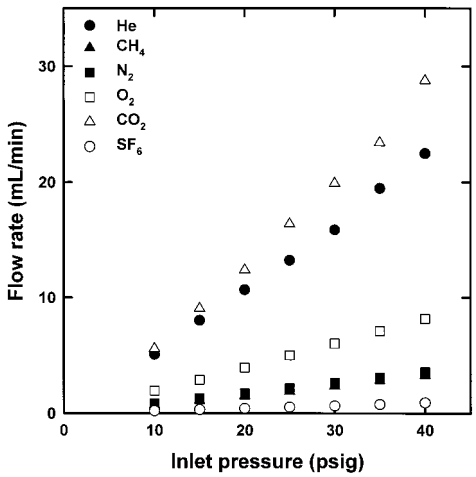

Figure 8. Flow rates of several gases through a fluorinated three-layer PAA film on gold-coated (5 nm) porous alumina (0.02-μm pore diameter) as a function of inlet pressure. The membrane area was 2.8 cm^2. Permeability values with standard deviations are listed in the text.

subsequent PAA layers, which should increase coverage, does not improve selectivity. We tested gas permeabilities of four-, five-, and six-layer PAA films. Four- and five-layer PAA films still showed Knudsen-like selectivities, and six-layer PAA film permeabilities were below the limit of detection of our flowmeter. The fact that additional PAA layers do not improve selectivity suggests that the lack of selectivity in these films is likely a property of hyperbranched PAA and not a manifestation of defects in substrate coverage by these films.

Derivatization of PAA films with $H_2NCH_2(CF_2)_6CF_3$ probably increases selectivities because of differing solubilities of gases in these films. Formation of a more crystalline membrane may also increase selectivity. The O_2/N_2 selectivities we observe with fluorinated PAA agree well with selectivities of other fluorinated membranes. Several studies report higher O_2 permeability values and improved O_2/N_2 selectivities (2−6) in a variety of fluorinated polymers such as fluorine-containing polydimethoxysilane (PDMS)-trimethylsilylpropyne (PTMSP) block copolymers, polyimides containing trifluoromethyl groups, and fluorine-containing PDMS-ethyl cellulose graft copolymers.[33−38] Aoki et al. also showed that adding a small amount (1 wt %) of poly(trifluoromethyl substituted arylacetylene) to PDMS and PTMSP films enhances oxygen permeability and O_2/N_2 selectivity.[39] The increased oxygen permeability of fluorinated membranes is most likely due to the high solubility of oxygen in fluorinated hydrocarbons.[39,40] CO_2/CH_4 selectivities of fluorinated PAA are also similar to those in a recent report on gas permeation through the fluorinated polymer poly(2,2-bis(trifluoromethyl)-4,5-difluoro-1,3-dioxole-*co*-tetrafluoroethylene (TFE/BDD87).[41]

Control experiments show that the selectivity shown by fluorinated PAA membranes is due to the film on the surface of the membrane and not to growth inside the pores. After attempted growth of a three-layer PAA film on a control sample (no MUA was deposited prior to PAA grafting), flux was too high to be measured by our flowmeter ($\gg$50 mL/min). After deposition of a six-layer PAA film on a control sample, flux was still higher than that for a three-layer PAA film grown with a MUA monolayer. These six-layer PAA films did not show selectivity (not even Knudsen selectivity), even after fluorination. As mentioned earlier, FESEM analysis of control samples did not show blocking of pores or the presence of a film on the surface. This shows that the presence of a monolayer is required for film growth on the surface and effective coverage of pores. Additionally, any growth inside the pores is not affecting permeability results.

We calculated permeability coefficients for three-layer PAA membranes using equation 1 and assuming a film thickness of 20 nm. The film thickness was estimated based on the thickness of three-layer PAA films on gold-coated silicon wafers and FESEM images of PAA films on gold-coated porous alumina. The permeability coefficients for the various gases are He, 2.6 $\pm$ 0.7 barrer; N_2, 1.4 $\pm$ 0.6 barrer; SF_6, 1.1 $\pm$ 0.5 barrer; O_2, 1.3 $\pm$ 0.6 barrer; CO_2, 1.3 $\pm$ 0.7 barrer; and CH_4, 2.0 $\pm$ 0.8 barrer; where 1 barrer is [10^{-10} cm^3 (STP) cm/(cm^2 s cm(Hg)]. In calculating the permeability coefficients of fluorinated films, we used a thickness of 40 nm because film thickness doubles upon fluorination with $H_2NCH_2(CF_2)_6CF_3$.[29] After fluorination, the permeability coefficients are higher for CO_2 (24 $\pm$ 3 barrer), He (20 $\pm$ 4 barrer), O_2 (7 $\pm$ 2 barrer), and N_2 (3.1 $\pm$ 0.7 barrer), whereas coefficients for CH_4 (2.9 $\pm$ 0.4 barrer) and SF_6 (0.8 $\pm$ 0.1 barrer) are relatively unchanged. The permeability coefficients are 10−50 times higher than those for a highly selective, ultrathin, conducting polymer membrane,[11] but about 2 orders of magnitude lower than those reported by Merkel et al. for TFE/BDD87.[41] The relatively low fluxes through fluorinated PAA may be due to crystallinity resulting from interactions between fluorinated octyl groups. We note that Teflon has a low permeability.[41]

Conclusions

The graft-on-graft synthesis and derivatization of PAA on gold-coated porous alumina yields selective, ultrathin membranes. Film thickness increases nonlinearly with the number

(33) Aoki, T. *Prog. Polym. Sci.* **1999**, *24*, 951−993.
(34) Coleman, M. R.; Koros, W. J. *J. Membr. Sci.* **1990**, *50*, 285−297.
(35) Nagase, Y.; Ochiai, J.; Matsui, K.; Uchikura, M. *Polym. Commun.* **1988**, *29*, 10−13.
(36) Nagase, Y.; Ochiai, J.; Matsui, K.; Uchikura, M. *Polymer* **1988**, *29*, 740−745.
(37) Kim, T. H.; Koros, W. J.; Husk, G. R.; OBrien, K. C. *J. Membr. Sci.* **1988**, *37*, 45−62.
(38) Stern, S. A.; Mi, Y.; Yamamoto, H. *J. Polym. Sci., Polym. Phys. Ed.* **1989**, *27*, 1887−1909.
(39) Aoki, T.; Oikawa, E.; Hayakawa, Y.; Nishida, M. *J. Membr. Sci.* **1991**, *57*, 207−216.
(40) Inagaki, N.; Kawai, H. *J. Polym. Sci., Polym. Chem. Ed.* **1986**, *24*, 3381−3391.
(41) Merkel, T. C.; Bondar, V.; Nagai, K.; Freeman, B. D.; Yampolskii, Y. P. *Macromolecules* **1999**, *32*, 8427−8440.

of deposited layers and these films effectively cover porous substrates, presumably because of their hyperbranched structure. FESEM and AFM images clearly show that six-layer PAA films cover the surface without filling underlying pores. Gas-permeability measurements indicate that three-layer PAA films show modest Knudsen diffusion-based selectivity, but fluorination of these films provides selective, ultrathin membranes for gas separations. Although the complex synthesis of hyperbranched PAA films will likely prohibit their use in commercial gas separations, these permeability data do show that PAA membranes can be defect-free and easily derivatized. Thus, PAA membranes might prove valuable in small-scale sensing or separations applications.

Acknowledgment. We acknowledge partial support of this work from the National Science Foundation (CHE-9816108), the Department of Energy (Division of Chemical Sciences, Office of Basic Energy Research), an ACS-PRF starter grant, and Michigan State University and its Center for Fundamental Materials Research. We thank the Keck microfabrication facility for use of instrumentation.

Supporting Information Available: External reflection FTIR spectra of one to six layers of PAA on gold-coated (63 nm) porous alumina, transmission FTIR spectrum of a three-layer PAA film on porous alumina along with a spectrum of the same film after fluorination, FESEM image (cross-section taken without gold-coating prior to imaging) of a four-layer PAA film grown on a gold-coated (63 nm) porous alumina membrane. This material is available free of charge via the Internet at http://pubs.acs.org.

JA002203T